# Investigation of the thermal conductivity of shape-modulated silicon nanowires by the Monte Carlo method combined with Green–Kubo formalism

I M Nkenfack, Mykola Isaiev, G. Pernot, D. Lacroix

# Investigation of the thermal conductivity of shape-modulated silicon nanowires by the Monte Carlo method combined with Green-Kubo formalism

I.M. Nkenfack,[a] M. Isaiev,[b] G. Pernot,[c] and D. Lacroix[d]
*Université de Lorraine, CNRS, LEMTA, Nancy F-54000, France*

(Dated: May 22, 2024)

In this study, we conducted calculations to determine the thermal conductivity of silicon nanowires with various shapes and cross-sectional designs using the Monte Carlo method combined with Green-Kubo heat flow autocorrelation. This computational approach is known for its reliability in predicting thermal properties of complex nanostructured devices. We specifically examined nanowires with circular or rectangular sections combined to complex serpentine and fishbone modulations. Our findings indicate that the nanowire's geometry significantly impacts the phonon mean free path and thermal transport. More specifically, patterns with serpentine modulations exhibit a pronounced reduction in thermal conductivity attributable to enhanced phonon boundary scatterings. Our simulation results are compared with available experimental data, highlighting the potential of our method for structural optimization in thermal management applications, particularly in devices like thermoelectric converters.

The study of heat transfer and the control of the thermal properties of nanostructured materials is of prime interest in a large number of applied domains. For example, in the field of nanoelectronics, the increasing downsizing of electronic components is hindered by the need to control and dissipate heat in the devices. A better understanding of heat transfer mechanisms at small time and space scales is therefore essential. At these scales, macroscopic approaches based on Fourier formalism are questionable. Wave or ballistic phenomena can dominate under certain conditions, depending on the size of the objects and the materials considered[1]. In practice, coherence effects are weak near room temperature in semiconductors. But, they may be important at low temperatures, when the wavelength of heat carriers is large compared to the size of the structure. However, if coherence effects are difficult to observe, nanostructuring makes possible to control the mean free path of phonons (MFP), i.e. vibrations that drive energy in semiconductors, and to tailor the thermal conductivity (TC) of engineered systems.

In the last few years, major advances have led to the development of new semiconductors, at micrometric scales, for which nanostructuring can be used to finely tune their transport properties. Objects such as Si nanoporous membranes[2] are a well-known example of observed thermal conductivity reduction in microscale devices compared to bulk Si. Moreover, experimental studies combining the elaboration and the characterization of nanowires (NW), for different geometries (size, shape, etc.), lead to the same conclusion. The latter have been investigated for a long time by various research groups such as the one of A. Majumdar[3] and the one of P. Yang[4]. However, in these studies, NW shapes were often regular while more complex patterning recently elaborated, in group of M. Nomura[5], which opened new application fields where rectification, Levy transport or localization are specific behaviour that may be encountered. There is also great interest in the use of diameter-modulated nanowires to improve the thermoelectric efficiency of devices. X. Zianni[6,7] highlights the unique capability of these nanowires to modify electron and phonon transport properties, thus improving thermoelectric effects and reducing phonon thermal conduction. She introduces the concept of "Thermoelectric metamaterial" (THEMMs) and explores Bayesian approaches to optimize aperiodicity in width-modulated nanowires, aiming to minimize phonon transmission and thermal conductance. Moreover, they discuss how some phonon modes are trapped in these nanowires, resulting in a significant reduction in the phonon heat flux rendering them promising new candidates for thermoelectric materials or thermal insulators. For low temperatures, Blanc et al.'s[8] research focuses on "corrugation" or shape modulation, which reduces the phonon mean free path (MFP) in silicon nanowires, leading to a decreased heat transfer. Recent studies by T. Hori[9] and Y. Song, along with G. Wehmeyer[10], delve into tuning thermal conductivity in nanowires through

[a] Electronic mail: isibert-marcel.nkenfack@univ-lorraine.fr
[b] Electronic mail: mykola.isaiev@univ-lorraine.fr
[c] Electronic mail: gilles.pernot@univ-lorraine.fr
[d] Electronic mail: david.lacroix@univ-lorraine.fr (Author to whom correspondence should be addressed)

structural modulation and employ ray tracing simulations to quantify phonon boundary scattering in complex modulated nanowires and diameter-modulated coaxial cylindrical nanowires, respectively. Overall, these works underscore the potential of nanowire's shape-modulation for controlling heat transport through structural optimization and seeking major improvements in device's efficiency such as thermoelectric energy conversion efficiency. They rely on various numerical techniques, highlighting the importance of simulation tools as a complementary approach to experimental research.

Regarding numerical studies, theoretical works on phonon transport in nanowires are mostly based on atomistic approaches (molecular dynamics calculations, MD), on the resolution of the Boltzmann transport equation (BTE)[11], or even o, "finite element" (FE) approaches. Works based on the use of non-equilibrium MD provide a realistic view of the induced thermal transport. However, when larger systems are considered, the requested computational resources are much more important than when using MC methods. For FE modeling, classical elasticity equations are solved, it gives access to the band structure of the considered objects[12,13]. However, these calculations remain limited to low temperatures. Eventually, solution of BTE, which is at the core of this work, will be discussed hereafter as it is a powerful approach to deal with realistic microstructured devices.

This letter discusses of heat transfer within nanowires with various shapes using a methodology based on Monte Carlo method to solve the BTE combined with Green-Kubo formalism (MC-GK). In our previous work[14], we developed an approach to evaluate the thermal conductivity of nanostructured systems. In the present letter, we apply this methodology to the assessment of the thermal conductivity of nanowires with different shapes and sizes, for an extended temperature range.

Specifically, we considered nanowires with circular or rectangular bases and others modulated as presented in Fig. 1. The wires (A) and (B), which respectively have cylindrical geometries of circular section (diameter $D$) and rectangular section (sides $L_x$ and $L_y$), let us define equivalent diameters as a function of the perimeter $D_{eq-P} = (2L_x + 2L_y)/\pi$, or the equivalent section $D_{eq-S} = 2\sqrt{(L_x \times L_y)/\pi}$. It allows us to compare the thermal conductivity of these NW assuming an equivalent volume or scattering surface area. For complex configurations, the wires (C), (D) and (E), also plotted in Fig. 1 have geometries with a rectangular section (ribbon shape). The wire (C) is a "serpentine" type characterized by two characteristic lengths, $L_{xm}$ defining the amplitude of the modulation and $L_{zm}$ representing the length of the modulation with $N_z = L_{zm}/L_z$, where $N_z$ is the number of modulations per unit length. For the wire (C), the cross-section remains constant. The wire (D) uses the same characteristic lengths $L_{xm}$ and $L_{zm}$, but the pattern of the wire has "sinusoidal" constrictions along the $z$ axis. Finally, the wire (E) corresponds to a "fishbone" modulated profile with two distinct cross-sections.

Assuming a corpuscular approach, phonon transport's dynamic is governed by the BTE (Eq. 1), which is solved in this study using the MC method. Phonons are considered as heat carrier particles with defined frequencies and polarizations. They are treated as classical energy packets that can move and collide within the nanostructure over time.

$$\frac{df}{dt} + \nabla_{\mathbf{K}\omega} \cdot \nabla_{\mathbf{r}} f = \frac{\partial f}{\partial t}_{\text{collisions}} \quad (1)$$

$f(\mathbf{K}, p, \mathbf{r}, t)$ is the distribution function, describing the probability to find a heat carrier with a certain energy and wave vector ($\mathbf{K}$) at a given position ($\mathbf{r}$) in space. The left-hand term of Eq. 1 corresponds to the phonon "transport" term, while the right-hand term characterizes the "intrinsic" scattering mechanisms that take into account processes involving 3-phonons interactions as well as those with the material impurities/defects. The nature of these mechanisms depends on the material (see supp. mat.). In the present work, Si phonon properties such as dispersion and lifetimes follow the bulk formalism as all characteristic lengths remain large enough ($L_{x,y,z}$ or $D >> 10$ nm.). In addition, in the considered temperature range, 3-phonon processes are sufficient to describe all the cases discussed in this work. Apart from that, it shall be noted that in our methodology, there is no "boundary" relaxation time, the latter scattering process is considered through phonon reflections on the edges of the nanowires.

The resolution of the BTE by MC method is an iterative process consisting of: i) an initialization phase, ii) the displacement of the carriers through the structure, taking into account potential reflections at the boundaries. In our case, we model diffuse reflections. In the explored temperature range, for a typical roughness of few nm, phonon reflections are mostly diffuse (see sup. mat.). Thus, we have considered the latter assumption to reduce the overall simulation time. To this end, reflections are treated by selecting a random vector in the half-hemisphere containing the normal to the collision surface. The reflected vector $\mathbf{R}$ is defined as follows:

$$\mathbf{R} = \cos(\theta) \cdot \mathbf{n} + \sin(\theta) \cdot (\cos(\phi)\mathbf{T}_1 + \sin(\phi)\mathbf{T}_2) \quad (2)$$

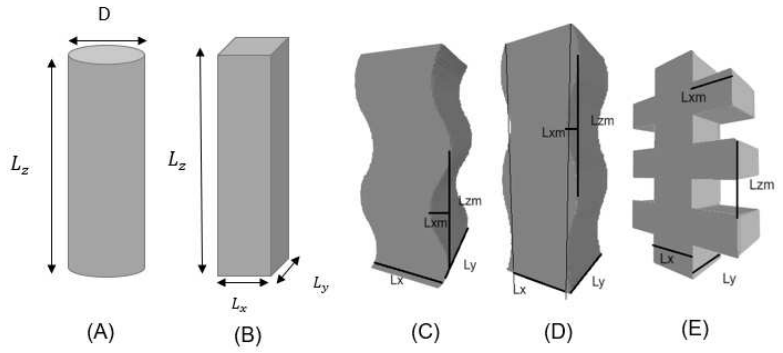


Figure 1. (NW-A) nanowire with circular base. (NW-B) nanowire with rectangular base. (NW-C) "serpentine" modulations (no constriction).(NW-D) "sinusoidal" modulations with constrictions. (NW-E) "fishbone" modulations with constrictions.

where $\theta$ is between $[0,\ \pi/2]$. The $\cos(\theta)$ is calculated using Lambert's law[15]: $\cos(\theta)=\sqrt{R_1}$, where $R_1$ is a number drawn randomly between 0 and 1. The angle $\phi$ is equal to $2\pi R_2$, where $R_2$ is drawn randomly between 0 and 1. $\mathbf{T}_1$ and $\mathbf{T}_2$ are normalized vectors tangential to the reflection surface such as $(\mathbf{T}_1 \perp \mathbf{T}_2 \perp \mathbf{n})$. At the edges of the system, along the $z$ axis, periodic conditions are set. iii) the possible occurrence of a scattering process (N or U or I), during a time step $\delta t$ based on a phonon lifetime $\tau$ at a given frequency and temperature, can be written as $P_{scat} = 1 - \exp(-\delta t/\tau(\omega, T))$[16]. iv) Finally, the calculations of the properties such as energy, temperature and heat flux are carried out. Steps ii) to iv) are repeated for a $N_t$ number of time steps defined at the beginning of the simulation. At this stage, it should be noted that no temperature gradient is imposed in the system studied, as is often the case with the MC method[17] and the simulations are carried out at a uniform temperature. As a result, the TC of the system is evaluated differently than the usual Fourier law. We use the so-called "Green-Kubo" (GK) formulation[16] to determine the system's TC tensor by calculating the flux autocorrelation.

$$k_{\alpha,\beta} = \frac{V}{k_B T^2} \int_0^\infty < q_\alpha(0) q_\beta(t) > dt \qquad (3)$$

where $V$ is the volume of the system, $\alpha$ and $\beta$ are the Cartesian coordinates of TC tensor $\overline{\overline{k}}$ and $\mathbf{q}$ $(q_x, q_y, q_z)$ is the heat flux. The specific aspects of Green-Kubo formalism, employed in this work, are given by Schelling and al.[18].

The temperature-dependent TC of nanowires (A, B, C, D and E) is computed with the MC-GK method. Details concerning discretization, time step and other general simulation inputs are given in the supp. mat. A sensitivity analysis about TC calculated values versus the number of sampled particles is also provided. Results are compared to experimental data provided in[3,12,19]. The graphs (1), (2), and (3) provided in Fig. 2 show the classical temperature dependence observed in bulk silicon[20], despite intrinsically lower values. This first observation demonstrates the significant impact of nanostructuring on the TC of silicon nanowires and the ability of the MC-GK method to capture this feature. In Fig. 2-(1), MC-GK simulations are done considering both assumptions of equivalent perimeter or equivalent cross section. The TC predictions are in agreement, since the relative errors obtained are less than 13% compared with experimental measurements. The simulation results of the NW-A match the experimental data for all considered temperatures. For low temperatures ($T < 250K$), results based on the equivalent perimeter $D_{eq-P}$ fit more accurately with the experimental data. When the temperature increases ($T > 250K$), those using $D_{eq-S}$ are closer to the measurements. This observation suggests that the decrease of temperature, which leads to an increase of phonon mean free path[21], induces TC variations driven by diffusion at the boundaries through nanostructuration[22,23]. In the latter case, it makes the assumption of an equivalent perimeter (i.e. transport dominated by boundary scattering) more accurate. Conversely, as $T$ increases, the MFP becomes smaller and the TC is varying according to both intrinsic and boundary scattering events. In order to assess the boundary scattering impact on thermal transport for all the considered structures, ray tracing simulations (RT) were carried out. In RT calculations, a large number of packets $(N_{\text{total}}(\omega, p))$ of pulsation $\omega$ and polarization $p$ phonons are sampled, and the number of collisions $N_{\text{BC}}(\omega, p)$ with

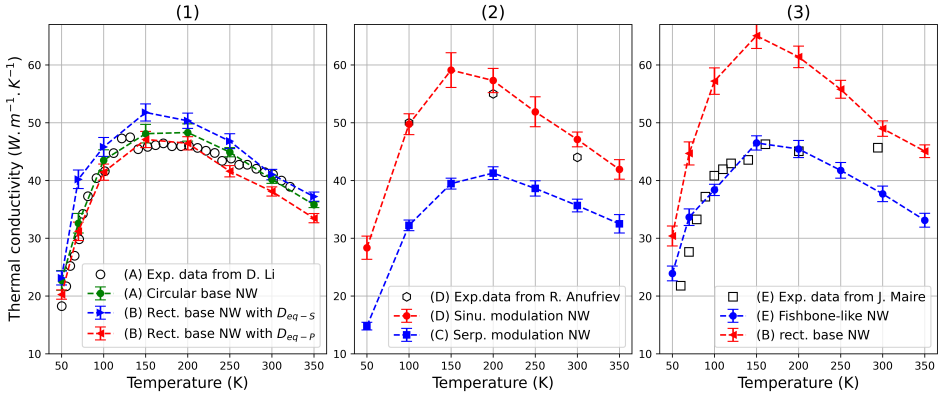


Figure 2. **Thermal conductivity as function of temperature:** (1) Experiments by Li et a.[3] NW-A with $D$=115 nm and MC-GK simulations of NW-A with the same characteristics and NW-B ($D_{eq-S}$: $L_x$=$L_y$=102 nm and $D_{eq-P}$: $L_x$=$L_y$=90 nm). (2) Experiments by Anufriev et al.[19] of NW-D, with characteristics: $L_x$=172 nm, $L_y$=145 nm, $L_z$=5 $\mu$m, $L_{xm}$=72.5 nm, $L_{zm}$=290 nm and MC-GK simulations of nanowires NW-C and NW-D with the same characteristics. (3) Experiments by Maire et al.[12] NW-E with lengths $L_x$=122 nm, $L_y$=145 nm, $L_{xm}$=190 nm, $L_{zm}$=186 nm and MC-GK simulations of NW-E with the same characteristics and straight nanowire (NW-B) with $L_x$=122 nm, $L_y$=145 nm.

the walls is recorded over short time intervals ($\Delta t$=1 ps). Thus, following a method similar to the one described by Lacroix and al.[24], it is possible to evaluate the boundary scattering MFP using :

$$MFP_{RT}(\omega,p) = \frac{V_g(\omega,p)\Delta t}{\ln\left(\frac{N_{\text{total}}(\omega,p)}{N_{\text{total}}(\omega,p)-N_{\text{BC}}(\omega,p)}\right)} \quad (4)$$

where $V_g$ represents the group velocity. Our simulation results can be compared to the general formulation proposed by Blanco and Fournier[25] which states that random diffusion processes in a close domain can be defined as $4V/S$, $V$ being the domain volume and $S$ the boundary surface. The results of the MFP calculations based on ray tracing, defined by the Eq. 4 and the theoretical ones for NW (B, C, D and E) are presented in Tab. I, both well agree. In addition, it can be seen that according to the chosen geometrical pattern and for similar characteristic lengths, the serpentine nanowire (NW-C) induces the strongest reduction of MFP. Similarly, the "fishbone" geometry also reduces MFP compared to a pristine nanowire even if this reduction remains weak. In the case of sinus-like shape, no reduction is observed as the geometry varies smoothly which may avoid phonon trapping. Another way to understand the transport in such structures is to probe the angular distribution of the phonon propagation directions. To this end, we consider NW (B, C, D and E) with a characteristic size given in Tab. I and a total length of $L_z = 2 \times L_{zm}$. Phonon transport procedure by MC method is the one used for TC evaluation and boundary scatterings remain purely diffuse. In this example, all "particles" are launched at $z = 0$ according to a Lambertian distribution and we record their propagation direction at $z = L_z/2$ and $z = L_z$. The idea is to observe how phonons are back-scattered in these systems and how many of them reach the upper limit of the structure. Yet, it shall be noticed that this simulation does not intend to compute TC of such particular systems but to observe the impact of the modulation pattern on carriers' displacements. Fig. 3 provides a polar representation of the phonon global propagation pattern. In the case of a straight NW, 26% of the launched phonons propagate through the nanostructure and the forward and backward propagation patterns are explicitly in the direction close to the NW $\mathbf{e}_z$ axis. On this basis, it can be seen that all the modulated geometries (C, D and E) further affect thermal properties as the amount of transmitted phonon falls to an average of 17.5%. There is a clear reduction of the transported energy in presence of shape modulation. In addition, from those calculations, it appears that specific NW geometry design can help to focus the phonon flow. For instance, in NW-E, the transmitted phonons remain in a smaller solid angle than in any other configurations. These observations combined with MFP calculation, done on experimental structures[3,12,19] and reported in Tab. II, will be used to discuss the TC results.

Fig. 2-(2) shows the results of nanowires with "serpentine" (C) and "sinusoidal" (D) shapes. Both have similar characteristics, the relative error between NW-D calcu-

lations and measurements[19] is lower than 6%. Furthermore, a strong decrease of the thermal conductivity is observed for the nanowire with a "serpentine" configuration (C) compared to the sinusoidal case (D). This decrease stems from the geometric design of the "serpentine" configuration, which induces more scattering at the boundaries despite equivalent geometric parameters.

Besides, in such "serpentine" NW, the open channel, that allows the phonon flow along $\mathbf{e}_z$ axis, may be reduced to further enhance TC lowering. Such results were recently observed in kinked nano-ribbons[26] where a TC decrease of about 20% was observed at room temperature between straight and kinked patterns. Those data are consistent with the present simulations.

| Nanowire | B | C | D[19] | E |
|---|---|---|---|---|
| $4V/S$ (nm) | 157.4 | 147.8 | 173.1 | 153.5 |
| $MFP_{RT}$ (nm) | 158±5 | 149±4 | 174±5 | 153 ±6 |

Table I. Values of MFP at room temperature in NW (B, C, D and E) with: $L_x = 172\ nm$, $L_y = 145\ nm$, and for modulated geometries $L_{xm} = 72.5\ nm$, $L_{zm} = 290\ nm$. D case is taken from Anufriev et al.[19]

| Nanowire | B[3] | B[3] | E[12] | B[12] |
|---|---|---|---|---|
| Size (nm) | $L_x$=102, $L_y$=102 | $L_x$=90, $L_y$=90 | $L_x$=122, $L_y$=145 | $L_x$=122, $L_y$=145 |
| Modulation (nm) | | | $L_{xm}$=190, $L_{zm}$=186 | |
| $4V/S$ (nm) | 102 | 90 | 119.9 | 132.5 |

Table II. Values of MFP at room temperature in NW (B-E) corresponding to Fig. 2. B and E cases are taken from[3,12]

.

In Fig. 2-(3), the "fishbone" type nanowire (E) developed in Nomura's group and the straight nanowire (B) with equivalent characteristics are considered. For NW-E, TC results agree with the experimental ones[12]. The impact of the "fishbone" design is obvious and a significant reduction of TC in NW-E can be noted compared to the constant cross-section case (NW-B). Agreement with measurements is very good from 50 to 200K. The TC decrease is related to the increase of boundary scattering. In addition, the "fishbone" geometry confines the heat carriers, reducing their transport within the nanostructure (see Tab. II). These observations have already been made in 2- and 3-dimensional interconnected nanowire arrays[27].

To conclude on these first TC results as a function of $T$ for different wire (ribbon) shapes, it appears that boundary scattering condition and its impact on the MFP can be directly related to the TC variations.

Further investigations explore the influence, at room temperature, of the system size (perimeter and cross-section) of simple nanowire (cases A and B), as well as the impact of the nanowire's length for cases B, C, D and E. Fig. 4-(1) and Fig. 4-(2) illustrate, in agreement with the experimental observations[3,4,28,29], the increase of the nanowire's TC as their perimeters or cross-sections become larger. For both types of nanowires (circular and square cross-section), the simulation results agree with the experimental ones with relative deviations below 5%. As observed previously in Fig. 2-(1), close to room temperature, the equivalent base perimeter and base cross-section are parameters that can be used to discuss TC variations as scattering mechanisms both depend on boundaries and intrinsic collisions.

The last studied case, plotted in Fig. 4-(3) provides the TC variations as a function of length $L_z$ for both straight and modulated nanowires (cases B, C, D and E). $L_z$ ranges from 700 nm to 5 $\mu$m. For these calculations, the total length of the wire is equal to $L_z = N_m \times L_{zm}$ with $N_m$ the number of modulations. The simulation results of the nanowire with sinusoidal modulations (NW-D) follow the experimental data from Anufriev's work[19] on a nanowire of the same geometry with relative errors of less than 10%.

In this study, we demonstrate the ability of the Monte Carlo method combined with Green Kubo formalism to evaluate the thermal properties of nanowires, moving from simple to much more complex geometries. Following a previous work[14], which addresses the issue of heat carrier transport in nanoporous materials, we have extended this approach to nanowires. This method offers several improvements over the works published in the literature based on the classical Monte Carlo method[22,30], including the ability to: directly extract the thermal conductivity tensor of the system, perform calculations at a prescribed temperature, increase the computing efficiency when phonon scattering is dominant. The latter point stems to the usually long simulation times required to reach steady-state with methods based on the Fourier's formalism, compared to methods using the heat flux autocorrelation. In addition, it gives the ability to track each "heat carrier" in the studied system to investigate, for example, their mean free path or the scattering behavior. Besides, the results obtained from the simulations (MC-GK) have been successfully compared to experimental data taken from different research groups, demonstrating the effectiveness of the modeling approach. Currently, the method also suffers some limitations (larger simulation times) when very low temperatures are considered and ballistic transport is dominant. Improvements of the MC-GK method are expected on both modelling and technical aspects. On the "modelling" side, we aim to take advan-

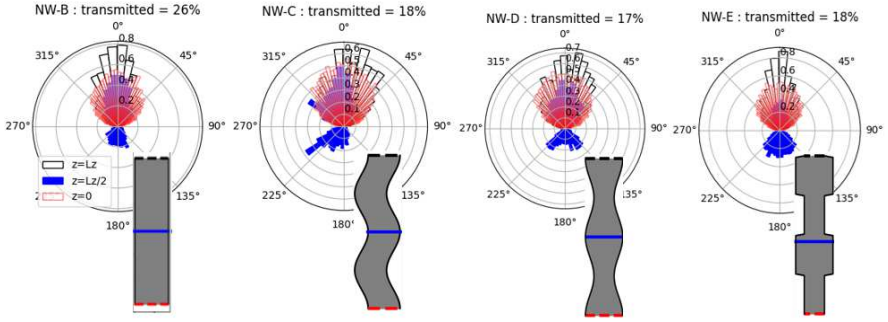


Figure 3. **Phonon propagation directions and transmission rates** for NW (B, C, D and E) with characteristic lengths reported in Tab. I and $L_z = 2 \times L_{zm}$. All sampled particles are launched at $z = 0$ and normalized polar plots of phonon angular distribution are computed at $z = 0$, $z = L_z/2$ and $z = Lz$

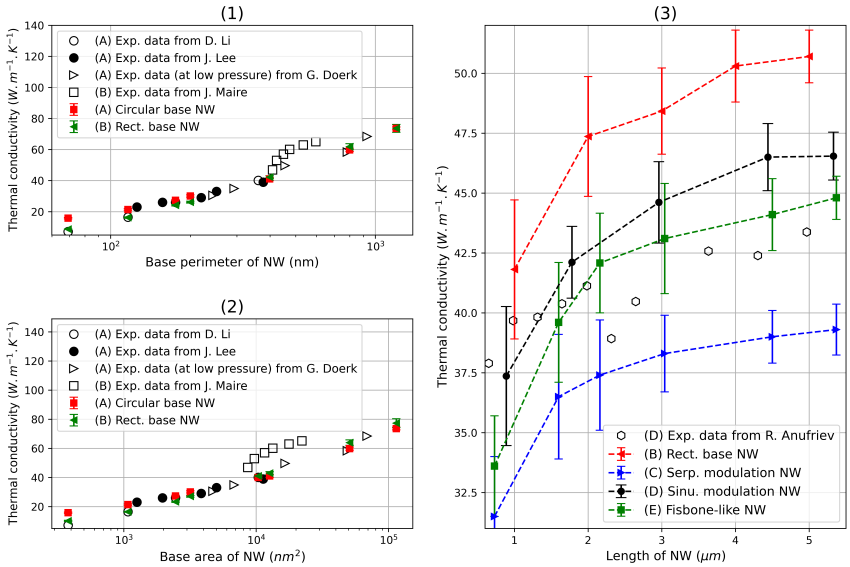


Figure 4. **Thermal conductivity at 300 K as a function of the size:** (1) TC variations with NW's perimeter (NW-A) and (NW-B). (2). TC variations with NW's cross-section (NW-A) and (NW-B). (3) TC variations with length $L_z$, (NW-D) with characteristics $L_x$=172 nm, $L_y$=145 nm, $L_{xm}$=72.5 nm, $L_{zm}$=290 nm and NW-B, NW-C, NW-D, NW-E with similar characteristics. Experimental data by[3,4,19,28,29].

tage of phonon tracking to investigate ballistic-diffusive transitions in nanostructures. On the "technical" side, we are considering tools to allow MC-GK calculations on GPU system in order to improve computing efficiency.

## ACKNOWLEDGMENTS

This paper contains results obtained in the frame of the project "SPiDER-man" (ANR-18-CE42-0006). This work was performed using HPC resources provided by the EXPLOR center hosted by the Université de Lorraine. Partially, this work was performed using HPC resources from GENCI-TGCC and GENCI-IDRIS through the project eDARI # A0130913052 and A0150913052.

## I. SUPPLEMENTARY MATERIAL

In the supplementary material, details of the calculation of phonon properties (dispersion and relaxation time) are given. In addition, details concerning the simulation parameters (geometries, sampling, time steps, etc.) are also given and their impact quantified. Finally, a sensitivity study on the impact of wire's roughness on transport is provided.

## REFERENCES

[1]G. Pernot, M. Stoffel, I. Savic, F. Pezzoli, P. Chen, G. Savelli, A. Jacquot, J. Schumann, U. Denker, I. Mönch, C. Deneke, O. G. Schmidt, J.M. Rampnoux, S. Wang, M. Plissonnier, A. Rastelli, S. Dilhaire, and N. Mingo. Precise control of thermal conductivity at the nanoscale through individual phonon-scattering barriers. Nature materials, 9:491–5, 06 2010.

[2]D. Song and G. Chen. Thermal conductivity of periodic microporous silicon films. Appl. Phys. Lett., 84(5):687–689, 01 2004.

[3]D. Li, Y. Wu, P. Kim, L. Shi, P. Yang, and A. Majumdar. Thermal conductivity of individual silicon nanowires. Appl. Phys. Lett., 83(14):2934–2936, 09 2003.

[4]J. Lee, W. Lee, J. Lim, Y. Yu, Q. Kong, J. Urban, and P. Yang. Thermal transport in silicon nanowires at high temperature up to 700 k. Nano lett., 16, 05 2016.

[5]R. Anufriev, S. Gluchko, S. Volz, and M. Nomura. Probing ballistic thermal conduction in segmented silicon nanowires. Nanoscale, 11:13407–13414, 2019.

[6]Xanthippi Zianni. Diameter-modulated nanowires as candidates for high thermoelectric energy conversion efficiency. Applied Physics Letters, 97(23):233106, 12 2010.

[7]Xanthippi Zianni. Thermoelectric metamaterials: Nanowaveguides for thermoelectric energy conversion and heat management at the nanoscale. Advanced Electronic Materials, 7(8):2100176, 2021.

[8]Christophe Blanc, Ali Rajabpour, Sebastian Volz, Thierry Fournier, and Olivier Bourgeois. Phonon heat conduction in corrugated silicon nanowires below the Casimir limit. Applied Physics Letters, 103(4):043109, 07 2013.

[9]Takuma Hori. Role of geometry and surface roughness in reducing phonon mean free path and lattice thermal conductivity of modulated nanowires. International Journal of Heat and Mass Transfer, 156:119818, 2020.

[10]Yingru Song and Geoff Wehmeyer. Maximizing and minimizing the boundary scattering mean free path in diameter-modulated coaxial cylindrical nanowires. Journal of Applied Physics, 130(4):045104, 07 2021.

[11]J. Zou and A. Balandin. Phonon heat conduction in a semiconductor nanowire. J. Appl. Phys., 89(5):2932–2938, 03 2001.

[12]Jeremie Maire, Roman Anufriev, Takuma Hori, Junichiro Shiomi, Sebastian Volz, and Masahiro Nomura. Thermal conductivity reduction in silicon fishbone nanowires. Scientific Reports, 8:4452, 03 2018.

[13]Zhigang G., Jian Y., Zhoutuo T., Xing T., Shang Z., and Qiuwang W. A simplified finite volume method for effective thermal conductivity in discrete particles. Powder Technology, 375:521–532, 2020.

[14]D. Lacroix, M. I. Nkenfack, G. Pernot, and M. Isaiev. Thermal properties of nanoporous materials, large scale modelling with the use of monte carlo phonon transport autocorrelation. J. Appl. Phys., 134(2):025101, 07 2023.

[15]K. Kukita and Y. Kamakura. Monte carlo simulation of phonon transport in silicon including a realistic dispersion relation. J. Appl. Phys., 114(15):154312, 10 2013.

[16]D. Lacroix, M. Isaiev, and G. Pernot. Thermal transport in semiconductors studied by monte carlo simulations combined with the green-kubo formalism. Phys. Rev. B, 104:165202, Oct 2021.

[17]D. Lacroix, K. Joulain, and D. Lemonnier. Monte carlo transient phonon transport in silicon and germanium at nanoscales. Phys. Rev. B, 72:064305, Aug 2005.

[18]P.K. Schelling, S.R. Phillpot, and P. Keblinski. Comparison of atomic-level simulation methods for computing thermal conductivity. Phys. Rev. B, 65:144306, Apr 2002.

[19]R. Anufriev, S. Gluchko, S. Volz, and M. Nomura. Quasi-ballistic heat conduction due to lévy phonon flights in silicon nanowires. ACS Nano, 12, 11 2018.

[20]Y.S. Touloukian, R.W. Powell, C.Y. Ho, P.G. Klemens, Thermophysical, and electronic properties information analysis center Lafayette In. Thermophysical Properties of Matter - The TPRC Data Series. Volume 1. Thermal Conductivity - Metallic Elements and Alloys. Defense Technical Information Center, 1970.

[21]R. Gereth and K. Hubner. Phonon mean free path in silicon between 77 and 250k. Phys. Rev., 134:A235–A240, Apr 1964.

[22]V. Jean, S. Fumeron, K. Termentzidis, X. Zianni, and D. Lacroix. Monte carlo simulations of phonon transport in si nanowires with constrictions. Int. J. of Heat and Mass Trans., 86:648–655, 07 2015.

[23]A. Malhotra and M. Maldovan. Impact of phonon surface scattering on thermal energy distribution of Si and SiGe nanowires. Scientific reports, 6:25818, 05 2016.

[24]D. Lacroix, K. Joulain, D. Terris, and D. Lemonnier. Monte carlo simulation of phonon confinement in silicon nanostructures: Application to the determination of the thermal conductivity of silicon nanowires. Appl. Phys. Lett., 89, 09 2006.

[25]S. Blanco and R. Fournier. An invariance property of diffusive random walks. Europhys. Lett., 61:168, 01 2007.

[26]S. Qiao, D. Li, and L. Yang. Heat flow guiding and modulation by kinks in a silicon nanoribbon. Nano Letters, 23(19):8860–8867, 2023.

[27]M. Verdier, D. Lacroix, and K. Termentzidis. Thermal transport in two- and three-dimensional nanowire networks. Phys. Rev. B, 98:155434, Oct 2018.

[28]J. Maire and M. Nomura. Reduced thermal conductivities of si one-dimensional periodic structure and nanowire. Jap. J. Appl. Phys., 53:06JE09, 05 2014.

[29]Gregory S. Doerk, Carlo Carraro, and Roya Maboudian. Single nanowire thermal conductivity measurements by raman thermography. ACS Nano, 4(8):4908–4914, 2010. PMID: 20731463.

[30]J.-P. Peraud, C. Landon, and N. Hadjiconstantinou. Monte carlo methods for solving the boltzmann transport equation. An. Rev. of Heat Trans., 17:205–265, 01 2014.